HHS Public Access

Author manuscript

J Autism Dev Disord. Author manuscript; available in PMC 2021 August 01.

Published in final edited form as:

J Autism Dev Disord. 2020 August ; 50(8): 2765–2778. doi:10.1007/s10803-020-04383-w.

Autism spectrum disorder symptoms are associated with connectivity between large-scale neural networks and brain regions involved in social processing

Korey P. Wylie[a], **Jason R. Tregellas**[a,b], **Joshua J. Bear**[c,d], **Kristina T. Legget**[a]

[a]Department of Psychiatry, University of Colorado School of Medicine, Anschutz Medical Campus, Fitzsimons Building, Mail Stop F546, 13001 East 17th Place, Aurora, CO 80045, USA.

[b]Research Service, Rocky Mountain Regional VA Medical Center, Eastern Colorado Health System, 1700 N. Wheeling St., Aurora, CO 80045, USA.

[c]Department of Pediatrics, Section of Neurology, Children's Hospital Colorado, 13123 East 16th Avenue, Aurora, CO 80045, USA.

[d]Department of Pediatrics, University of Colorado School of Medicine, Anschutz Medical Campus, 13123 East 16th Avenue, Aurora, CO 80045, USA.

Abstract

The neurobiology of autism spectrum disorder remains poorly understood. The present study addresses this knowledge gap by examining the relationship between functional brain connectivity and Autism Diagnostic Observation Schedule (ADOS) scores using publicly available data from the Autism Brain Imaging Data Exchange (ABIDE) database (N=107). This relationship was tested across all brain voxels, without *a priori* assumptions, using a novel statistical approach. ADOS scores were primarily associated with decreased connectivity to right temporoparietal junction, right anterior insula, and left fusiform gyrus (p<0.05, corrected). Seven large-scale brain networks influenced these associations. Findings largely encompassed brain regions involved in

Correspondence concerning this article should be addressed to: Kristina T. Legget, PhD, University of Colorado Anschutz Medical Campus, 13001 E. 17th Pl., Mail Stop F546, Fitzsimons Building, Room E4315, Aurora, CO 80045, Phone: (303) 724-5809, Kristina.Legget@ucdenver.edu.

Korey P. Wylie, M.D., Department of Psychiatry, University of Colorado School of Medicine, Anschutz Medical Campus, Fitzsimons Building, Mail Stop F546, 13001 East 17th Place, Aurora, CO, 80045, USA.

Jason R. Tregellas, Ph.D., Department of Psychiatry, University of Colorado School of Medicine, Anschutz Medical Campus, Fitzsimons Building, Mail Stop F546, 13001 East 17th Place, Aurora, CO, 80045, USA. Research Service, Rocky Mountain Regional VA Medical Center, Eastern Colorado Health System, 1700 N. Wheeling St., Aurora CO, 80045, USA.

Joshua J. Bear, M.D., Department of Pediatrics, Section of Neurology, Children's Hospital Colorado; Department of Pediatrics, University of Colorado School of Medicine, Anschutz Medical Campus, 13123 East 16th Avenue, Aurora, CO 80045, USA.

Kristina T. Legget, Ph.D., Department of Psychiatry, University of Colorado School of Medicine, Anschutz Medical Campus, Fitzsimons Building, Mail Stop F546, 13001 East 17th Place, Aurora, CO, 80045, USA.

Conflict of Interest: The authors declare that they have no conflict of interest.

Compliance with Ethical Standards:

Ethical approval: All procedures performed in studies involving human participants were in accordance with the ethical standards of the institutional and/or national research committee and with the 1964 Helsinki declaration and its later amendments or comparable ethical standards.

Informed consent: Informed consent was obtained from all individual participants included in the study.

processing socially relevant information, highlighting the importance of these processes in autism spectrum disorder.

Keywords

ADOS; ABIDE; Distance Covariance; Independent Components Analysis; Functional Connectivity

Understanding the neurobiology of autism spectrum disorders (ASD) remains a formidable challenge for psychiatry. Exploratory studies have investigated the neurobiology underlying ASD symptoms by correlating Autism Diagnostic Observation Schedule (ADOS) scores with functional magnetic resonance imaging (fMRI)-measured connectivity metrics, or neural features observable with other neuroimaging modalities. The ADOS, often considered the “gold-standard” in ASD diagnostics (Mehling and Tasse 2016), is a semi-structured assessment of naturalistic social interactions, communication and imaginative play (Lord et al. 2000). Associations between ADOS scores and neuroimaging metrics have proven difficult to replicate, however, likely due to small sample sizes or inconsistencies and biases introduced by the use of regions-of-interest that are chosen *a priori* and differ across studies (Lord and Jones 2012; Muller et al. 2011). To date, the neurobiology associated with ASD symptoms has not been investigated with an approach that addresses these issues, such as a data-driven, comprehensive, whole-brain analysis, with a large sample of subjects, rigorously corrected for multiple comparisons.

In the current investigation, we examined the neurobiology of ASD symptoms, as assessed via the ADOS, using resting state fMRI scans from the Autism Brain Imaging Data Exchange (ABIDE). ABIDE is a large, multicenter aggregate of neuroimaging and phenotypic data from participants with ASD and matched controls, directed and coordinated by Drs. Adriana Di Martino and Michael Milham (Di Martino et al. 2014). The current study comprehensively investigated the association between ADOS scores and brain connectivity, at the voxel level, using a novel statistical approach involving a combination of independent components analysis (ICA) and distance covariance (dCov). ICA is a dimension reduction technique that, when applied to fMRI data, can identify spatial patterns of voxels showing covariation over time that can be easily interpretable as neural processing systems, e.g. large-scale brain networks. dCov is a recently-developed multivariate technique, validated for use in large-scale association studies, that yields greater statistical power and flexibility, relative to more commonly-used correlation measures (Simon and Tibshirani 2014; Székely et al. 2007). In contrast with classical statistical methods such as multiple regression, dCov is applicable even when substantial multicollinearity exists (i.e., predictor variables are correlated with each other), when the number of predictor variables exceeds the sample size, or when statistical assumptions regarding the distribution of random variables, such as normality of residuals, do not hold (Székely et al. 2007). As will be described below, combining dCov with ICA allows us to improve the biological interpretability of results, while minimizing the problems associated with the large dimensionality of the data.

The aim of the current study was to investigate how brain connectivity relates to ASD symptoms, using a novel combination of statistical approaches to enhance both replicability

and biological/clinical interpretability. Given that deficits in social communication and interaction are core ASD symptoms (American Psychiatric Association, 2013), we suggest that the neural systems and regions that process social information, often called the "social brain," may provide a promising framework in which to investigate the neurobiology of ASD. The social brain is a network of interconnected regions specialized for processing socially relevant information. These include the temporoparietal junction (TPJ), medial prefrontal cortex (mPFC), orbitofrontal cortex, and amygdala (Adolphs 2003; Frith 2007). More recently, additions to the social brain include the anterior insula (aIns), due to its involvement in empathy, as well as the fusiform gyrus, due to its involvement in processing facial expressions (Adolphs 2009). Both structural and functional abnormalities have been observed in these social processing regions in individuals with ASD (Mason et al. 2008; Di Martino et al. 2009; Redcay et al. 2013; Hernandez et al. 2015; Patriquin et al. 2016).

In the current study, we tested two hypotheses. First, based on recent meta-analyses of abnormal neural activity during social tasks in participants with ASD (Di Martino et al. 2009; Patriquin et al. 2016), we hypothesized that ADOS scores would be associated with connectivity involving the right TPJ, bilateral fusiform gyrus, aIns, and amygdala. Second, because ASD has not been shown to be associated with abnormal connectivity to any single region or network, we hypothesized that the association between ADOS scores and connectivity would differ depending on the specific region and connection, such that regional heterogeneity would be observed in terms of the large-scale networks that influence each region.

Methods

Participants

ABIDE is a multi-site aggregate of functional and structural MRI data, accompanied by extensive phenotypic information, including ADOS scores (Di Martino et al. 2014). The ABIDE I data release, which was used in the current study, consists of 1,112 subjects. Of these, 539 had a diagnosis of ASD and 573 were classified as typically developing. Specific diagnostic criteria for each site can be found at the ABIDE website: http://fcon_1000.projects.nitrc.org/indi/abide/abide_I.html.

All data were anonymized in accordance with HIPAA guidelines. Collection and sharing of data was carried out with the approval of the local Institutional Review Boards for all participating sites, with all data obtained following informed consent. Details on the informed consent process, IRB approval and site-specific protocols can also be found at the ABIDE website: http://fcon_1000.projects.nitrc.org/indi/abide/.

Inclusion criteria for the current investigation largely followed the criteria of Di Martino et al. (Di Martino et al. 2014) and consisted of the following: (i) successful registration with near full brain coverage in all anatomical and resting state scans, as assessed manually; (ii) reported full-scale IQ of greater than 70; (iii) available resting-state scan with minimum duration of five minutes; (iv) mean framewise displacement no more than 2 SD above sample mean (mean=0.08, SD=0.04); (v) ADOS scores available, calculated using the Gotham algorithm (selected due to its improved diagnostic validity compared to previous

algorithms (Gotham et al. 2007; Oosterling et al. 2010)); (vi) data collected at a site with more than ten subjects, after applying the above criteria. This resulted in 107 subjects across four sites, with an age range of 7–19 years (see Table 1 for demographic information). The majority of these subjects were administered ADOS module 3 (n=103), with a few completing module 2 (n=3). Information regarding the ADOS module administered was not available for one subject.

fMRI Data Preprocessing

Preprocessed resting-state fMRI data were acquired from the ABIDE website (Craddock et al., 2013; http://preprocessed-connectomes-project.org/abide/index.html). Data were preprocessed using the DPARSF pipeline (http://preprocessed-connectomes-project.org/abide/dparsf.html). As per this pipeline, all volumes were corrected for differences in slice timing during acquisition, realigned using a six-parameter linear transform, registered to anatomical scans using a rigid body transform, and registered to the first volume as well as the mean of the images. The first four volumes were discarded from analyses to allow for stabilization of the magnetic field. The effects of head motion were regressed out using a 24-parameter model, as were nuisance signals from white matter and cerebrospinal fluid. Following nuisance regression, linear and quadratic trends were removed using band-pass frequency filtering (0.01–0.1 Hz), and smoothed with a 6 mm full width at half maximum (FWHM) Gaussian kernel. Global signal was not removed.

Independent Components Analysis (ICA)

The number of independent signals in the dataset was estimated using bootstrap stability analysis (BSA) of principal components (Majeed and Avison 2014). BSA is a data-driven method of selecting the expected number of independent components by comparing the stability of group-level principal components under bootstrap resampling to the stability of simulated Gaussian noise with the same shape, dimensions, and preprocessing pipeline as the original data. Compared to information-theoretic methods, such as minimum description length (MDL) criteria, BSA is resistant to overfitting due to noise in the data and preprocessing steps such as frequency filtering (Majeed and Avison 2014). BSA estimated at most 36 independent source signals that significantly differed from Gaussian noise in the reduced, concatenated subject data.

Following model order estimation with BSA, group ICA was carried out using GIFT v3.0b (http://mialab.mrn.org/software/gift/). The 36 components were extracted using the infomax algorithm (Bell and Sejnowski 1995). Voxel time series were whitened, variance normalized, and temporally concatenated with two principal component analysis (PCA) data reduction steps, of 70 and 36 components. Spatial maps were reconstructed with GICA3 and scaled to z-scores (Erhardt et al. 2011). All spatial maps and time courses were visually inspected to identify noise components. Seven components, classified as artifacts based on spatial distributions in cerebrospinal fluid (CSF), white matter, or high-frequency oscillations, were excluded from further analysis. To identify common intrinsic connectivity networks (ICNs), group mean ICA spatial maps were correlated with published ICN templates (Shirer et al. 2012). Templates matching multiple ICA components were classified as subnetworks based on anatomical differences, while ICA components without template matches were classified

based on anatomy. Following group ICA, whole-brain networks were back-reconstructed individually for each subject in order to investigate associations with that subject's clinical symptoms.

Subject-level Whole-brain Network Construction

Next, back-reconstructed ICN time series were correlated with each voxel's time series in a functional connectivity analysis (Figure 1). The resulting vector of bivariate simple correlations for each voxel represents the set of extrinsic inputs and outputs unique to that voxel, which has been termed its "connectional fingerprint" (Passingham et al. 2002). In this context, connectivity refers to a voxel's interactions with the entire neural processing system, or large-scale networks identified with ICA, rather than its connectivity with another voxel. Each voxel's connectional fingerprint, or connectivity vector, was subsequently tested for association with ADOS scores, after removing the influences of sex, age, full-scale IQ, mean framewise displacement, and site, using linear regression residuals (Hua et al. 2015).

Behavioral Associations with Voxels

Distance covariance (dCov) is a recently-developed multivariate technique that tests the statistical independence of two vectors with arbitrary dimensions (Székely et al. 2007). The dCov statistic is zero if and only if the random vectors are independently distributed, but is increasingly positive otherwise. Compared to similar techniques (e.g., mass univariate Pearson correlations, maximal information coefficient), dCov has demonstrated increased statistical power for identifying associations in large datasets (Simon and Tibshirani 2014).

dCov analyses in the current study proceeded in two steps. First, dCov was calculated for each grey matter voxel, using subjects' connectivity vectors and ADOS total scores as inputs (Figure 1). This resulted in an unthresholded whole-brain statistical map, showing associations between voxel-level connectivity and ADOS total scores in the sample. Results were corrected for multiple comparisons using a modification of Nichols' cluster-level non-parametric test (Nichols and Holmes 2002). 5,000 volumes were generated by permuting subjects' ADOS total scores for each voxel. Empirical p-values were calculated as the proportion of times the permutation dCov statistic exceeded the original dCov statistic at that voxel. For the permutation volumes, empirical p-values for all voxels were calculated in an identical manner. All volumes were then thresholded using a cluster-defining threshold (CDT) of $p<0.005$. Lastly, resulting cluster sizes were calculated. In the original (i.e., non-permutation) thresholded whole-brain statistical map, a cluster was considered significant after correcting for multiple comparisons if the empirical p-value of obtaining a cluster this size or larger was significant at $p<0.05$. Significant clusters were displayed as cortical surface projections, created using Caret version 5.65 (Van Essen et al. 2001).

Networks Contributing to Behavioral Associations

To better understand the specific elements of the connectivity vector that contributed to each voxel's significance in the whole-brain analysis, dCov was used to test connectivity of the elements of the vector individually, using an individual scalar correlation coefficient and the scalar ADOS total score as input (Figure 1). Resulting dCov statistics for each connection were thresholded and corrected for multiple comparisons using a cluster-level permutation

test, similar to that used in the preceding voxel-level association analysis. dCov was first applied to individual connections between a voxel and an ICN (Figure 1). Empirical p-values were then calculated and compared against a CDT. In contrast to the voxel-level analysis (see Behavioral Associations with Voxels section above), however, the definitions of "cluster" and "adjacent" in the context of a network are unclear. This discrepancy can be resolved using definitions provided by the field of graph theory. In graph theory, a connection is said to be adjacent to an ICN node if it is connected to it, e.g., if an edge between nodes i and j is denoted by the ordered pair (i, j), then it is adjacent to nodes i and j (Newman 2010). Using this definition, a cluster is defined as a set of adjacent connections. As such, cluster size is determined as the number of connections to an individual ICN ("unweighted degree" in graph theory terminology). With this definition, cluster size was calculated and compared to the null distribution from a non-parametric permutation test. An individual connection was considered significant, after correcting for multiple comparisons, if it was located within a cluster of significant size. In order to determine the ICNs influencing the association between ADOS scores and neuroanatomy, all significant voxels ($p<0.05$, corrected) in the voxel-level association analysis were analyzed in the network-level association analysis. dCov was calculated for each connection to every ICN. Each connection was thresholded with a CDT of $p<0.005$. The null distribution of the unweighted degree was calculated using 5,000 permutation networks and used to correct for multiple comparisons at the network level. An individual connection was considered significant, after correcting for multiple comparisons, if the degree of its adjacent ICN node was significant at $p<0.05$. Significant connections were displayed as two-dimensional sagittal, coronal, and axial projections in MNI space, in the "glass brain" format.

Directionality of Behavioral Associations

As noted above, dCov is zero if and only if behavioral measures are independent and increasingly positive otherwise. Similar to the absolute value of a correlation, positive and negative linear relationships are indistinguishable with this approach. Consequently dCov, by itself, does not provide information on whether connectivity is increased or decreased, only that patterns of connectivity are associated with patterns of ADOS scores. For example, an association identified by dCov could represent a negative linear relationship (i.e., hypoconnectivity), a positive linear relationship (i.e., hyperconnectivity), a combination of both positive and negative linear associations, or even a non-linear pattern of association. Consequently, the directionality of the relationship between connectivity and ADOS scores was examined using other established statistical methods in a post-hoc, exploratory analysis. Average connectivity between each ICN and all voxels within each of the regions of interest identified in the main analysis was calculated and entered as a predictor for ADOS scores in separate linear regression models.

Results

ICA and Intrinsic Connectivity Networks (ICNs)

Twenty-nine ICNs matched templates for known networks, including 14 networks commonly identified with resting state fMRI (Shirer et al. 2012) and several of their subnetworks (Supplementary Figure 1).

Neurobiology Contributing to ADOS Scores

Following ICA and network classification, each voxel's connectivity was tested for associations with ADOS scores using dCov in a comprehensive whole-brain analysis. Connectivity was primarily associated with ADOS scores in clusters located in the right aIns, right TPJ, left fusiform gyrus, middle frontal gyrus, and middle insula (Figure 2a and Table 2, all clusters significant at $p<0.05$, corrected). Additional smaller clusters of significant associations ($p<0.05$, corrected) were located in the precuneus, right parahippocampal gyrus and temporal pole, and left posterior insula.

Specific Network Connectivity Contributing to ADOS Scores

After brain regions in which connectivity was associated with ADOS scores were determined, the specific network or networks associated with ADOS scores in these regions was examined. For each voxel within these clusters, each connection to every ICN was tested for associations with ADOS scores using dCov. Resulting network clusters, or unweighted degree, were corrected for multiple comparisons using non-parametric permutation testing. Seven networks significantly contributed to the associations between ADOS scores and the regions identified in the whole-brain analysis (Figure 2b, all edges significant at $p<0.05$, corrected). Although additional networks were statistically significant, their influence was relatively minor and less focal in comparison. Consequently, although all identified networks (see Supplementary Figure 1) were included in the analysis, the discussion and display of results will focus on the seven most influential ones (Figure 3). These were as follows: the ventral Default Mode Network (vDMN; a network encompassing the precuneus and middle frontal gyri bilaterally); a Language subnetwork centered on the bilateral temporoparietal junction (Language-TPJ; note that two additional Language subnetworks were also identified, one centered on the middle temporal gyri (Language-MTG) and one on the inferior frontal gyri (Language-IFG)); the primary Visual network; two Sensorimotor networks (Left Sensorimotor (L SM) and medial Sensorimotor (med SM)); and two anterior Salience Network (aSN) subnetworks, one centered on the dACC and one centered on the aIns (aSN-dACC and aSN-aIns, respectively).

Associations between these ICNs and ADOS scores differed by anatomical region. Connectivity between the right TPJ and the vDMN, aSN-aIns, L SM, and primary Visual ICNs was associated with ADOS total score. However, in the aIns, the association with ADOS total score was influenced by a different set of ICNs that included the anterior Salience subnetworks aSN-aIns and aSN-dACC, as well as the Language-TPJ network and the vDMN. In contrast, in the left fusiform gyrus, ADOS total score was associated with connectivity to the primary Visual, Language-TPJ, L SM, and med SM networks. Thus, the influence of network connectivity on ADOS scores was not uniform, but instead varied by neuroanatomical region.

ADOS Subscales and Connectivity

Since ADOS total scores reflect both Social Affect and Restricted/Repetitive Behaviors subscales, we tested the individual contributions of the two subscales to the above results in an exploratory analysis. While results using the ADOS Social Affect subscale were nearly identical to those using ADOS total scores, in terms of associations to both neurobiology as

well as ICNs, the results for the ADOS Restricted/Repetitive Behaviors subscale differed widely. ADOS Social Affect scores were associated with connectivity between clusters in the right aIns, right TPJ, left fusiform gyrus, middle frontal gyrus, and middle insula (see Supplementary Figure 2). Within these regions, connectivity to the L SM, vDMN, aSN-dACC, aSN-aIns, and Language-TPJ networks influenced Social Affect scores with the same regionally specific pattern as the ADOS total scores. In contrast, ADOS Restricted/Repetitive Behaviors scores were associated with connectivity with clusters of voxels in the bilateral middle frontal gyri, right superior frontal gyrus, and right inferior parietal lobes. Within these regions, connectivity to the Visuospatial (VS), Precuneus (PrC), dorsal Default Mode (dDMN), as well as the Language-MTG and Language-IFG networks influenced Restricted/Repetitive Behaviors scores (see Supplementary Figure 3). These results suggest that, despite being a sum of the two subscales, associations observed between ADOS total scores and functional connectivity were more strongly influenced by the Social Affect subscale than the Restricted/Repetitive Behaviors subscale.

Directionality of Behavioral Associations

The preceding analysis identified regions of the brain and large-scale networks where connectivity is associated with ADOS scores. It did not, however, examine the pattern of these associations in terms of how increased or decreased connectivity relates to ADOS scores, as this cannot be tested directly with dCov (see Methods). As such, directionality of the associations between ADOS scores and connectivity was investigated using linear regression models in exploratory post-hoc analyses. These analyses focused on associations between ADOS scores and connectivity to the right aIns, right TPJ, and left fusiform gyrus, as these regions were included in our *a priori* hypothesis and were the regions in which the cluster size was greatest when determining where in the brain connectivity was associated with ADOS scores (see Figure 2a and Table 2).

All linear associations between ADOS total scores and all individual ICNs were negative in all three of these brain regions (right aIns, right TPG, left fusiform gyrus). As an example, connectivity to the left fusiform gyrus was negatively associated with ADOS scores in all seven ICNs examined (Figure 4). Similar patterns of negative associations were found for connectivity to the right TPJ and right aIns (see Supplementary Figures 4 & 5). Since this pattern was consistent, it can be more insightfully explored by averaging across networks, rather than considering each network's influence separately. Consequently, associations with ADOS scores, averaged across all seven networks, were examined using linear regression, with results displayed as scatterplots. In all three brain regions examined, higher ADOS scores (indicating more pronounced ASD-associated symptoms) were associated with decreased connectivity (Figure 5). All models (Figure 4; Supplementary Figures 4 & 5) showed relatively low coefficients of determination (r^2 <0.2), suggesting that the association with ADOS scores detected by dCov may not be a simple linear relationship. Furthermore, beyond these three regions of interest and seven ICNs, other regions and networks may show different patterns of associations between ADOS scores and connectivity. To investigate this possibility, an additional exploratory analysis was carried out in which individual correlations between ADOS scores and connectivity were calculated for all voxels and individual connections identified by dCov (i.e., all lines between voxels and ICNs displayed

in Figure 2b). Of the 365 connections displayed in Figure 2, 90% of edges were negatively correlated with ADOS scores. The overall distribution showed a predominantly negative relationship (Figure 6; mean correlation = −0.15, median = −0.16, range = −0.4 to 0.2). These results suggest that, in general, hypoconnectivity is associated with ADOS scores, at the voxel level, throughout almost all regions and connections within the brain.

Discussion

This study examined the relationship between functional connectivity and ASD symptoms, as measured by the ADOS, in a whole-brain voxel-level analysis. It builds upon previous analyses by using non-exploratory statistical methods and a large sample of subjects from multiple research sites. Furthermore, this study applied a recently-developed multivariate statistical technique, distance covariance (dCov), which allows for greater statistical power, compared to Pearson's correlation, to detect associations in large-scale datasets (Simon and Tibshirani 2014). By using dCov in conjunction with a data-driven dimension reduction technique (independent components analysis, ICA) to identify intrinsic brain networks, the current study aimed to optimize both reproducibility and interpretability of results. Reproducibility was also enhanced through the use of standardized preprocessing methods and the incorporation of a fully non-parametric cluster-level approach to multiple comparison correction. By applying these methods to the ABIDE dataset, this study aimed to comprehensively and reproducibly examine the relationship between symptoms and connectivity.

Results were largely consistent with our hypothesis regarding the neuroanatomic localization of ASD symptoms. That there were many regions in which connectivity was not observed to be associated with ADOS scores suggests that these findings are region-specific, rather than representing a global relationship between brain connectivity and symptoms. At a voxel-level, ADOS scores were associated with the right TPJ, right aIns, and left fusiform gyrus, as hypothesized (Figure 2, Table 2). How these results relate to the known functional neuroanatomy of the social brain may offer insight into the specific processing systems that contribute to ASD symptoms.

The right TPJ has been associated with many social processing systems, including those underlying theory of mind (Adolphs 2009; Hernandez et al. 2015). The observed negative correlation between connectivity and ADOS scores in this region (Figure 5) is consistent with disrupted theory of mind previously observed in ASD (Baron-Cohen et al. 1997; Kana et al. 2014). However, the right TPJ is not specific to theory of mind, but also is involved in shifts in attention, including during joint attention tasks, as well as facial processing (Krall et al. 2015; Redcay et al. 2012; Gobbini and Haxby 2007). Given this non-specific functional role of the right TPJ, the observed association with ADOS scores in this region could be indicative of symptoms involving multiple social processing systems.

Symptom scores were also associated with connectivity in the aIns, a high-level associative region that integrates multimodal sensory information, affect, and awareness (Craig 2009). Within the context of the social brain, this region has been associated with empathy, which is the capacity to share the emotional states of others (Singer 2006; Adolphs 2009). The

negative correlation between aIns connectivity and ADOS scores observed in the current study (Figure 5) is consistent with this interpretation, suggesting that disrupted aIns connectivity may impede sharing of emotional states during social interactions. aIns connectivity has previously been associated with symptoms related to sensory over-responsivity in ASD (Green et al. 2016). The negative correlation between aIns connectivity and ADOS scores observed here, however, does not directly support this interpretation. Instead, these results suggest that increased information flow to the aIns is associated with *fewer* symptoms related to ASD. Given that the current results did not involve sensory networks, this suggests that the symptoms captured by ADOS total scores may be distinct from symptoms related to sensory responsivity.

The third region identified in the analysis was the fusiform gyrus, a higher-level visual processing region that responds to faces and complex visual information (Schultz et al. 2003; Dziobek et al. 2010). The negative correlation observed between fusiform connectivity and ADOS scores in the current study (Figure 5) suggests a disconnected fusiform gyrus at rest, potentially impacting the ability to respond to socially relevant information. Interestingly, connectivity between the left fusiform gyrus and the medial Sensorimotor network (Figure 2) is reminiscent of a recent investigation of body language interpretation in individuals with ASD, in which the left fusiform gyrus and left paracentral lobule showed abnormal coherence in individuals with ASD during processing of emotionally evocative body postures (Libero et al. 2014). These findings suggest that during body language interpretation, individuals with ASD may encode low-level visual features (e.g., body shape, posture) abnormally. The current results suggest yet-unexplored contributions from this essential nonverbal form of communication to social interactions measured by the ADOS.

The current study found that different regional associations with ASD symptoms were influenced by connectivity to different networks (Figures 2 & 5). For example, in the right TPJ, ADOS scores were associated with connectivity to vDMN, aSN-aIns, and the primary Visual Network. However, in the left fusiform gyrus, ADOS scores were associated with connectivity to primary Visual, Language-TPJ and med SM networks. All regions were influenced by multiple ICNs and no single ICN influenced all regional associations between connectivity and symptoms. These results are consistent with our hypothesis that ADOS scores would show a regionally heterogeneous pattern in terms of how they relate to connectivity.

While the main analysis approach focused on ADOS total scores, analyses were also performed separately on the Social Affect and Restricted/Repetitive Behaviors subscales of the ADOS. A nearly identical set of anatomical clusters was observed to be influential in both the ADOS total score and ADOS Social Affect subscale score analyses, as were the same set of ICNs. Interestingly, a different set of clusters and networks were observed to influence ADOS Restricted/Repetitive Behaviors subscale scores. In this case, the analysis of subscales individually may provide more detailed information regarding the neurobiology underlying the different components of the ADOS, suggesting future utility in investigating how connectivity is associated with each subscale in subsequent studies.

Lastly, the current results are supportive of ASD symptoms being associated with hypoconnectivity, i.e., decreased information flow between brain networks and regions (Figures 5 & 6). This is consistent with many, though not all (e.g., see Muller et al. 2011; Hull et al. 2017) previous studies, which have reported ASD-associated resting-state hypoconnectivity involving a variety of regions, including those highlighted by the current study, such as the insula (Anderson et al. 2011; Ebish et al. 2011; von dem Hagen et al. 2013; Zhao et al. 2016), fusiform gyrus (Anderson et al. 2011; Gotts et al. 2012; Zhao et al. 2016), TPJ (Gotts et al. 2012; von dem Hagen et al. 2013), salience network (von dem Hagen et al. 2013; Abbott et al. 2016), and DMN (Kennedy and Courchesne, 2008; Assaf et al. 2010; Weng et al. 2010; von dem Hagen et al. 2013; Zhao et al. 2016; Hull et al. 2017). Because hypoconnectivity was associated with ADOS scores in specific regions of the cortex, not everywhere in the brain, and with connections to specific networks, not all large-scale networks, the present findings suggest that a more specific and fine-grained hypoconnectivity contributes to symptoms in ASD.

This analysis is limited by several factors. Distance covariance identifies patterns of multivariate associations, but does not provide information on the directionality of those associations. Consequently, the relationship between hypoconnectivity and ADOS scores was assessed with a post-hoc, exploratory analysis. The pre-selection of anatomical regions using dCov (e.g., right TPJ, right aIns, and left fusiform gyrus) likely upwardly biased the magnitude of associations to ADOS scores when subsequently explored in this post-hoc regression analysis. Additionally, other measures of ASD symptomology, such as the Social Responsiveness Scale (Constantino et al. 2003) and the Autism Diagnostic Interview (Rutter et al. 2003), may provide additional information regarding how connectivity relates to the severity of ASD symptoms, but were not evaluated in the present study. The ADOS was selected for the current analysis because it directly assesses observed behaviors (i.e., scores are based on direct observation by a trained clinician). It is unknown if the current results extend to other ASD-related measures, or to what extent their underlying neurobiologies overlap or potentially differ, and are worthy of future study. The Gotham algorithm scores used in the current study (Gotham et al. 2007) are a revision of the original ADOS scoring algorithm (Lord et al. 1999), designed to improve comparability across modules, with a reduction in impact of age or verbal IQ observed for modules 2 and 3 (Gotham et al. 2007; Gotham et al. 2009). Calibrated severity scores (CSS) were later developed to further improve comparability across modules and decrease influence of participant characteristics likely to differ among the different modules administered (e.g., age, verbal IQ) (Gotham et al. 2009). That almost all subjects included in the current analysis completed module 3 of the ADOS supports the use of the revised algorithm scores, rather than calibrated severity scores. The use of the ADOS as an outcome measure, and of non-calibrated scores, is also in fitting with previous studies investigating relationships between ASD symptoms and neurobiology (Assaf et al. 2010; Ecker et al. 2010; Poustka et al. 2011; Ecker et al. 2012; Keehn et al. 2012; Nair et al. 2013; Sato et al. 2013; Björnsdotter et al. 2016; Chen et al. 2016; Wei et al. 2018). Finally, while the inclusion of all subjects, rather than only those with an ASD diagnosis, helps us understand the biology of a set of behaviors, it does not necessarily address the difference in variability that would be expected between ASD and TD groups, which also merits further investigation.

In conclusion, the current study comprehensively investigated the relationship between functional connectivity and ADOS scores, in a whole-brain voxel-level analysis, using fMRI and a novel combination of ICA and dCov. Results suggest that ASD symptoms, as measured by the ADOS, are associated with connectivity alterations to many regions, particularly those involved in processing social information. Furthermore, connections to multiple networks influenced the relationship between connectivity and symptoms in these regions. These results suggest a richness and heterogeneity of connectivity within the brain as it relates to ASD symptoms, perhaps mirroring the clinical heterogeneity of ASD presentation.

Supplementary Material

Refer to Web version on PubMed Central for supplementary material.

Acknowledgments:

Funding: This work was supported by National Institutes of Health grants R01MH102224 (JRT), R01DK103691 (JRT), R21DK102052 (JRT), K01DK100445 (KTL), and UL1TR002535 (KTL/KW).

References

Abbott AE, Nair A, Keown CL, Datko M, Jahedi A, Fishman I, et al. (2016). Patterns of atypical functional connectivity and behavioral links in autism differ between default, salience, and executive networks. Cereb Cortex, 26(10), 4034–4045, doi:10.1093/cercor/bhv191. [PubMed: 26351318]

Adolphs R. (2003). Cognitive neuroscience of human social behaviour. Nat Rev Neurosci, 4(3), 165–178, doi:10.1038/nrn1056. [PubMed: 12612630]

Adolphs R. (2009). The social brain: neural basis of social knowledge. Annu Rev Psychol, 60, 693–716, doi:10.1146/annurev.psych.60.110707.163514. [PubMed: 18771388]

American Psychiatric Association. (2013). Diagnostic and Statistical Manual of Mental Disorders (5th ed.). Arlington, VA: American Psychiatric Pub.

Anderson JS, Nielsen JA, Froehlich AL, DuBray MB, Druzgal TJ, Cariello AN, et al. (2011). Functional connectivity magnetic resonance imaging classification of autism. Brain, 134, 3742–3754, doi:10.1093/brain/awr263. [PubMed: 22006979]

Assaf M, Jagannathan K, Calhoun VD, Miller L, Stevens MC, Sahl R, et al. (2010). Abnormal functional connectivity of default mode sub-networks in autism spectrum disorder patients. Neuroimage, 53(10), 247–256, doi:10.1096/j.neuroimage.2010.05.067. [PubMed: 20621638]

Baron-Cohen S, Jolliffe T, Mortimore C, & Robertson M. (1997). Another advanced test of theory of mind: evidence from very high functioning adults with autism or asperger syndrome. J Child Psychol Psychiatry, 38(7), 813–822. [PubMed: 9363580]

Bell AJ, & Sejnowski TJ. (1995). An information-maximization approach to blind separation and blind deconvolution. Neural Computation, 7(6), 1129–1159. [PubMed: 7584893]

Björnsdotter M, Wang N, Pelphrey K, & Kaiser MD. (2016). Evaluation of quantified social perception circuit activity as a neurobiological marker of autism spectrum disorder. JAMA Psychiatry, 73(6), 614–621. [PubMed: 27096285]

Chen H, Duan X, Liu F, Lu F, Ma X, Zhang Y, et al. (2016). Multivariate classification of autism spectrum disorder using frequency-specific resting-state functional connectivity—a multi-center study. Progress in Neuro-Psychopharmacology and Biological Psychiatry, 64, 1–9. [PubMed: 26148789]

Constantino JN, Davis SA, Todd RD, Schindler MK, Gross MM, Brophy SL, et al. (2003). Validation of a brief quantitative measure of autistic traits: Comparison of the social responsiveness scale

with the autism diagnostic interview-revised. J Autism Dev Disord, 33(4), 427–433. [PubMed: 12959421]

Craddock C, Benhajali Y, Chu C, Chouinard F, Evans A, Jakab AS, et al. (2013). The Neuro Bureau Preprocessing Initiative: open sharing of preprocessed neuroimaging data and derivatives. Frontiers in Neuroinformatics, doi:10.3389/conf.fninf.2013.09.00041.

Craig AD. (2009). How do you feel--now? The anterior insula and human awareness. Nat Rev Neurosci, 10(1), 59–70, doi:10.1038/nrn2555. [PubMed: 19096369]

Di Martino A, Ross K, Uddin LQ, Sklar AB, Castellanos FX, & Milham MP. (2009). Functional brain correlates of social and nonsocial processes in autism spectrum disorders: an activation likelihood estimation meta-analysis. Biol Psychiatry, 65(1), 63–74, doi:10.1016/j.biopsych.2008.09.022. [PubMed: 18996505]

Di Martino A, Yan CG, Li Q, Denio E, Castellanos FX, Alaerts K, et al. (2014). The autism brain imaging data exchange: towards a large-scale evaluation of the intrinsic brain architecture in autism. Mol Psychiatry, 19(6), 659–667, doi:10.1038/mp.2013.78. [PubMed: 23774715]

Dziobek I, Bahnemann M, Convit A, & Heekeren HR. (2010). The role of the fusiform-amygdala system in the pathophysiology of autism. Arch Gen Psychiatry, 67(4), 397–405, doi:10.1001/archgenpsychiatry.2010.31. [PubMed: 20368515]

Ebisch SJ, Gallese V, Willems RM, Mantini D, Groen WB, Romani GL, et al. (2011). Altered intrinsic functional connectivity of anterior and posterior insula regions in high- functioning participants with autism spectrum disorder. Hum Brain Mapp, 32(7), 1013–1028, doi:10.1002/hbm.21085. [PubMed: 20645311]

Ecker C, Rocha-Rego V, Johnston P, Mourao-Miranda J, Marquand A, Daly EM, et al. (2010). Investigating the predictive value of whole-brain structural MR scans in autism: a pattern classification approach. Neuroimage, 49(1), 44–56, doi:10.1016/j.neuroimage.2009.08.024. [PubMed: 19683584]

Ecker C, Suckling J, Deoni SC, Lombardo MV, Bullmore ET, Baron-Cohen S, et al. (2012). Brain anatomy and its relationship to behavior in adults with autism spectrum disorder: a multicenter magnetic resonance imaging study. Arch Gen Psychiatry, 69(2), 195–209, doi:10.1001/archgenpsychiatry.2011.1251. [PubMed: 22310506]

Erhardt EB, Rachakonda S, Bedrick EJ, Allen EA, Adali T, & Calhoun VD. (2011). Comparison of multi-subject ICA methods for analysis of fMRI data. Hum Brain Mapp, 32(12), 2075–2095, doi:10.1002/hbm.21170. [PubMed: 21162045]

Frith CD. (2007). The social brain? Philos Trans R Soc Lond B Biol Sci, 362(1480), 671–678, doi:10.1098/rstb.2006.2003. [PubMed: 17255010]

Gobbini MI, & Haxby JV. (2007). Neural systems for recognition of familiar faces. Neuropsychologia, 45(1), 32–41, doi:10.1016/j.neuropsychologia.2006.04.015. [PubMed: 16797608]

Gotham K, Risi S, Pickles A, & Lord C. (2007). The Autism Diagnostic Observation Schedule: revised algorithms for improved diagnostic validity. J Autism Dev Disord, 37(4), 613–627, doi:10.1007/s10803-006-0280-1. [PubMed: 17180459]

Gotham K, Pickles A, & Lord C. (2009). Standardizing ADOS scores for a measure of severity in autism spectrum disorders. J Autism Dev Disord, 39(5), 693–705, doi:10.1007/s10803-008-0674-3. [PubMed: 19082876]

Gotts SJ, Simmons WK, Milbury LA, Wallace GL, Cox RW, Martin A. (2012). Fractionation of social brain circuits in autism spectrum disorders. Brain, 135, 2711–2725, doi:10.1093/brain/aws160. [PubMed: 22791801]

Green SA, Hernandez L, Bookheimer SY, & Dapretto M. (2016). Salience network connectivity in autism is related to brain and behavioral markers of sensory overresponsivity. J Am Acad Child Adolesc Psychiatry, 55(7), 618–626 e611, doi:10.1016/j.jaac.2016.04.013. [PubMed: 27343889]

Hernandez LM, Rudie JD, Green SA, Bookheimer S, & Dapretto M. (2015). Neural signatures of autism spectrum disorders: insights into brain network dynamics. Neuropsychopharmacology, 40(1), 171–189, doi:10.1038/npp.2014.172. [PubMed: 25011468]

Hua WY, Nichols TE, Ghosh D, & Alzheimer's Disease Neuroimaging Initiative. (2015). Multiple comparison procedures for neuroimaging genomewide association studies. Biostatistics, 16(1), 17–30, doi:10.1093/biostatistics/kxu026. [PubMed: 24963012]

Hull JV, Dokovna LB, Jacokes ZJ, Torgerson CM, Irimia A, Van Horn JD. (2017). Resting-state functional connectivity in autism spectrum disorders: a review. Front Psychiatry, 7, 205, doi:10.3389/fpsyt.2016.00205. [PubMed: 28101064]

Kana RK, Libero LE, Hu CP, Deshpande HD, & Colburn JS. (2014). Functional brain networks and white matter underlying theory-of-mind in autism. Soc Cogn Affect Neurosci, 9(1), 98–105, doi:10.1093/scan/nss106. [PubMed: 22977198]

Keehn B, Shih P, Brenner LA, Townsend J, & Müller RA. (2013). Functional connectivity for an "island of sparing" in autism spectrum disorder: An fMRI study of visual search. Human brain mapping, 34(10), 2524–2537. [PubMed: 22495745]

Kennedy DP, Courchesne E. (2008). The intrinsic functional organization of the brain is altered in autism. Neuroimage, 39(4), 1877–1885, doi:10.1016/j.neuroimage.2007.10.052. [PubMed: 18083565]

Krall SC, Rottschy C, Oberwelland E, Bzdok D, Fox PT, Eickhoff SB, et al. (2015). The role of the right temporoparietal junction in attention and social interaction as revealed by ALE meta-analysis. Brain Struct Funct, 220(2), 587–604, doi:10.1007/s00429-014-0803-z. [PubMed: 24915964]

Libero LE, Stevens CE Jr., & Kana RK. (2014). Attribution of emotions to body postures: an independent component analysis study of functional connectivity in autism. Hum Brain Mapp, 35(10), 5204–5218, doi:10.1002/hbm.22544. [PubMed: 24838987]

Lord C, & Jones RM. (2012). Re-thinking the classification of autism spectrum disorders. J Child Psychol Psychiatry, 53(5), 490–509, doi:10.1111/j.1469-7610.2012.02547.x. [PubMed: 22486486]

Lord C, Risi S, Lambrecht L, Cook EH Jr., Leventhal BL, DiLavore PC, et al. (2000). The Autism Diagnostic Observation Schedule-Generic: a standard measure of social and communication deficits associated with the spectrum of autism. J Autism Dev Disord, 30(3), 205–223. [PubMed: 11055457]

Majeed W, & Avison MJ. (2014). Robust data driven model order estimation for independent component analysis of fMRI data with low contrast to noise. PLoS One, 9(4), e94943, doi:10.1371/journal.pone.0094943. [PubMed: 24788636]

Mason RA, Williams DL, Kana RK, Minshew N, & Just MA. (2008). Theory of Mind disruption and recruitment of the right hemisphere during narrative comprehension in autism. Neuropsychologia, 46(1), 269–280, doi:10.1016/j.neuropsychologia.2007.07.018. [PubMed: 17869314]

Mehling MH, & Tasse MJ. (2016). Severity of autism spectrum disorders: current conceptualization, and transition to DSM-5. J Autism Dev Disord, 46(6), 2000–2016, doi:10.1007/s10803-016-2731-7. [PubMed: 26873143]

Muller RA, Shih P, Keehn B, Deyoe JR, Leyden KM, & Shukla DK. (2011). Underconnected, but how? A survey of functional connectivity MRI studies in autism spectrum disorders. Cereb Cortex, 21(10), 2233–2243, doi:10.1093/cercor/bhq296. [PubMed: 21378114]

Nair A, Treiber JM, Shukla DK, Shih P, & Müller R-A. (2013). Impaired thalamocortical connectivity in autism spectrum disorder: a study of functional and anatomical connectivity. Brain, 136(6), 1942–1955. [PubMed: 23739917]

Newman M. (2010). Networks: An Introduction. New York: Oxford university press.

Nichols TE, & Holmes AP. (2002). Nonparametric permutation tests for functional neuroimaging: a primer with examples. Hum Brain Mapp, 15(1), 1–25. [PubMed: 11747097]

Oosterling I, Roos S, de Bildt A, Rommelse N, de Jonge M, Visser J, et al. (2010). Improved diagnostic validity of the ADOS revised algorithms: a replication study in an independent sample. J Autism Dev Disord, 40(6), 689–703, doi:10.1007/s10803-009-0915-0. [PubMed: 20148299]

Passingham RE, Stephan KE, & Kotter R. (2002). The anatomical basis of functional localization in the cortex. Nat Rev Neurosci, 3(8), 606–616, doi:10.1038/nrn893. [PubMed: 12154362]

Patriquin MA, DeRamus T, Libero LE, Laird A, & Kana RK. (2016). Neuroanatomical and neurofunctional markers of social cognition in autism spectrum disorder. Hum Brain Mapp, 37(11), 3957–3978, doi:10.1002/hbm.23288. [PubMed: 27329401]

Poustka L, Jennen-Steinmetz C, Henze R, Vomstein K, Haffner J, & Sieltjes B. (2012). Fronto-temporal disconnectivity and symptom severity in children with autism spectrum disorder. The World Journal of Biological Psychiatry, 13(4), 269–280. [PubMed: 21728905]

Redcay E, Dodell-Feder D, Mavros PL, Kleiner M, Pearrow MJ, Triantafyllou C, et al. (2013). Atypical brain activation patterns during a face-to-face joint attention game in adults with autism spectrum disorder. Hum Brain Mapp, 34(10), 2511–2523, doi:10.1002/hbm.22086. [PubMed: 22505330]

Redcay E, Kleiner M, & Saxe R. (2012). Look at this: the neural correlates of initiating and responding to bids for joint attention. Front Hum Neurosci, 6, 169, doi:10.3389/fnhum.2012.00169. [PubMed: 22737112]

Rutter M, Le Couteur A, & Lord C. (2003). Autism Diagnostic Interview-Revised. Los Angeles, CA: Western Psychological Services.

Sato JR, Hoexter MQ, Oliveira PP Jr., Brammer MJ, Consortium MA, Murphy D, et al. (2013). Inter-regional cortical thickness correlations are associated with autistic symptoms: a machine-learning approach. J Psychiatr Res, 47(4), 453–459, doi:10.1016/j.jpsychires.2012.11.017. [PubMed: 23260170]

Schultz RT, Grelotti DJ, Klin A, Kleinman J, Van der Gaag C, Marois R, et al. (2003). The role of the fusiform face area in social cognition: implications for the pathobiology of autism. Philos Trans R Soc Lond B Biol Sci, 358(1430), 415–427, doi:10.1098/rstb.2002.1208. [PubMed: 12639338]

Shirer WR, Ryali S, Rykhlevskaia E, Menon V, & Greicius MD. (2012). Decoding subject-driven cognitive states with whole-brain connectivity patterns. Cereb Cortex, 22(1), 158–165, doi:10.1093/cercor/bhr099. [PubMed: 21616982]

Simon N, & Tibshirani R. (2014). Comment on" Detecting novel associations in large data sets" by Reshef Et Al, Science Dec 16, 2011. arXiv preprint arXiv:1401.7645.

Singer T. (2006). The neuronal basis and ontogeny of empathy and mind reading: review of literature and implications for future research. Neurosci Biobehav Rev, 30(6), 855–863, doi:10.1016/j.neubiorev.2006.06.011. [PubMed: 16904182]

Székely GJ, Rizzo ML, & Bakirov NK. (2007). Measuring and testing dependence by correlation of distances. The Annals of Statistics, 35(6), 2769–2794.

Van Essen DC, Drury HA, Dickson J, Harwell J, Hanlon D, & Anderson CH. (2001). An integrated software suite for surface-based analyses of cerebral cortex. J Am Med Inform Assoc, 8(5), 443–459. [PubMed: 11522765]

von dem Hagen EA, Stoyanova RS, Baron-Cohen S, Calder AJ. (2013). Reduced functional connectivity within and between "social" resting state networks in autism spectrum conditions. Soc Cogn Affect Neurosci, 8(6), 694–701, doi:10.1093/scan/nss053. [PubMed: 22563003]

Wei L, Zhong S, Nie S, & Gong G. (2018). Aberrant development of the asymmetry between hemispheric brain white matter networks in autism spectrum disorder. European Neuropsychopharmacology, 28(1), 48–62. [PubMed: 29224969]

Weng SJ, Wiggins JL, Peltier SJ, Carrasco M, Risi S, Lord C, et al. (2010). Alterations of resting state functional connectivity in the default network in adolescents with autism spectrum disorders. Brain Res, 1313, 202–214, doi:10.1016/j.brainres.2009.11.057. [PubMed: 20004180]

Zhao Y, Chen H, Li Y, Lv J, Jiang X, Ge F, et al. (2016). Connectome-scale group-wise consistent resting-state network analysis in autism spectrum disorder. Neuroimage: Clinical,12, 23–33, doi:10.1016/j.nicl.2016.06.004. [PubMed: 27358766]

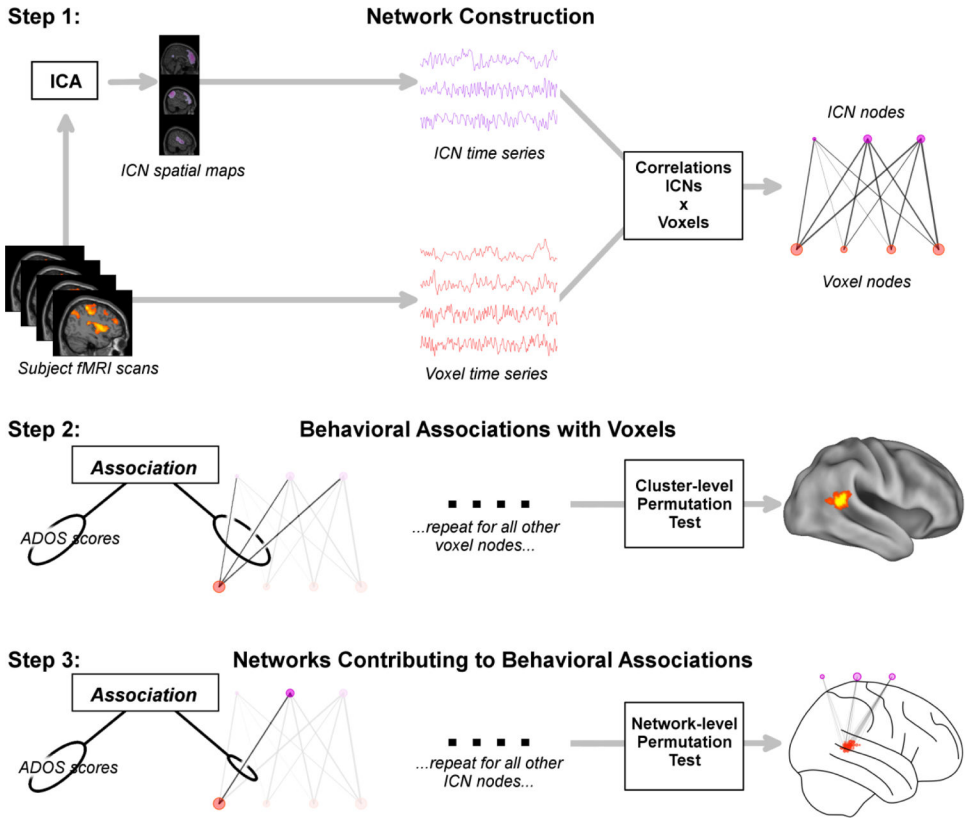

Figure 1.

Multi-level analysis steps. Step 1: Network construction. Following preprocessing, large-scale intrinsic connectivity networks (ICNs) were estimated using independent components analysis (ICA), resulting in a set of time series for each network. Each network's time series was then correlated with every voxel's time series, resulting in a bipartite network with voxel and ICN nodes (red and purple circles, respectively) efficiently summarizing and classifying all connectivity within the brain. Step 2: Behavioral associations with voxels. Each voxel's connectivity vector (all connections to a single red circle) was associated with Autism Diagnostic Observation Schedule (ADOS) scores using multivariate distance covariance (dCov). Statistical inference was carried out using a cluster-level permutation test. Resulting whole-brain spatial maps show *where* in the brain connectivity is associated with ADOS scores. Step 3: Networks Contributing to Behavioral Associations. Connectivity between each ICN and every significant voxel in the previous step was tested for associations with ADOS scores using dCov. Statistical inference was carried out using a network-level permutation test. Resulting bipartite graphs demonstrated *which* specific ICNs influence ADOS scores in each region.

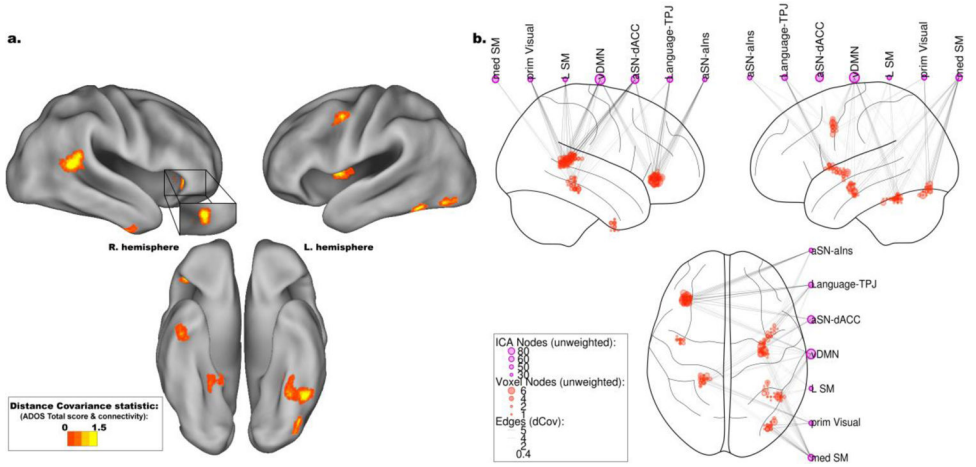

Figure 2.

Neuroanatomical and network associations between autism spectrum disorder symptoms and functional connectivity as measured by distance covariance (dCov). **a.** Throughout the entire brain, Autism Diagnostic Observation Schedule (ADOS) total score was primarily associated with connectivity to the right temporoparietal junction (TPJ) and anterior insula (aIns), as well as the left fusiform gyrus, middle frontal gyrus, and middle insula. Smaller clusters of association were in the right temporal pole and lingual gyrus, as well as left posterior insula and lateral occipital lobe.

b. Seven Intrinsic Connectivity Networks (ICNs), identified with Independent Components Analysis (ICA), primarily contributed to the neuroanatomical associations displayed in Figure 2a. These included medial and Left Sensorimotor networks (med SM and L SM, respectively), primary Visual (prim Visual), ventral Default Mode Network (vDMN), a Language subnetwork centered on the bilateral temporoparietal junction (Language-TPJ), and two subnetworks of the anterior Salience Network (aSN) centered on the dorsal Anterior Cingulate Cortex (aSN-dACC) and anterior insula (aSN-aIns). The influence of connectivity on these ICNs varied by region. The left fusiform gyrus was associated with ADOS total scores through its connections to prim Visual and med SM networks, while the aIns was associated with ADOS total scores through both aSN subnetworks, the vDMN, and the Language-TPJ network.

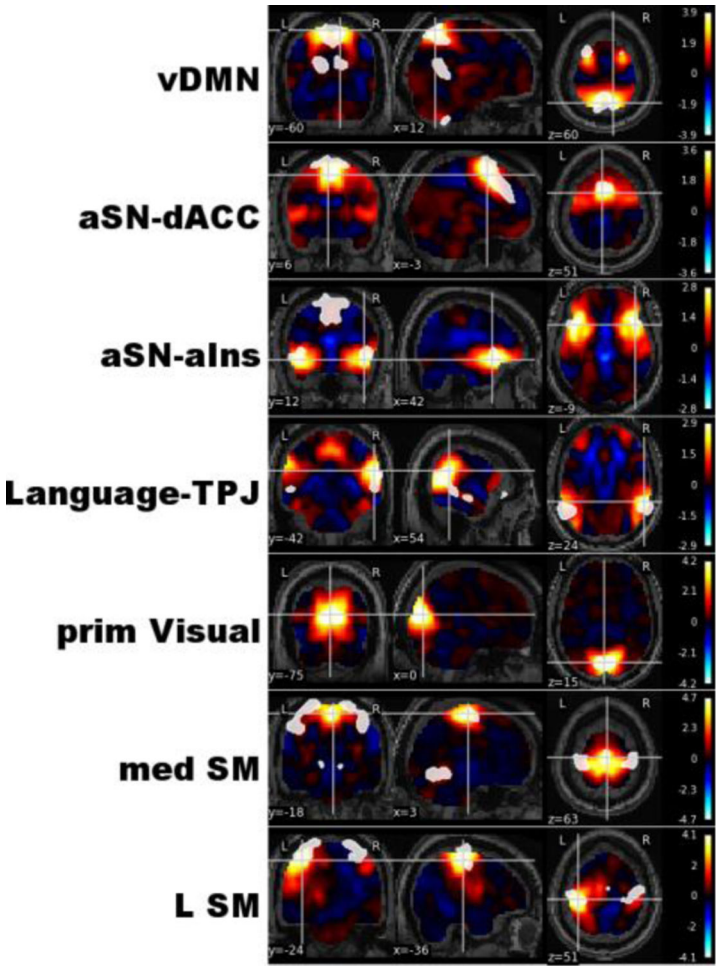

Figure 3.

Intrinsic connectivity networks relevant to autism spectrum disorder. Seven out of 29 intrinsic connectivity networks (ICNs) representing independent processing systems within the brain were associated with autism spectrum disorders. These included the ventral Default Mode Network (vDMN), two subnetworks of the anterior Salience Network centered on the dorsal Anterior Cingulate Cortex (aSN-dACC) and anterior insula (aSN-aIns), a subnetwork of the Language network centered on the bilateral temporoparietal junction (Language-TPJ), the primary Visual Network (prim Visual), as well as medial and Left Sensorimotor networks (med SM and L SM, respectively). X, Y, and Z coordinates are relative to Montreal Neurological Institute (MNI) space; weights from independent components analysis (ICA) are displayed in the legend, with binary templates for known ICNs plotted in white (Shirer et al. 2012).

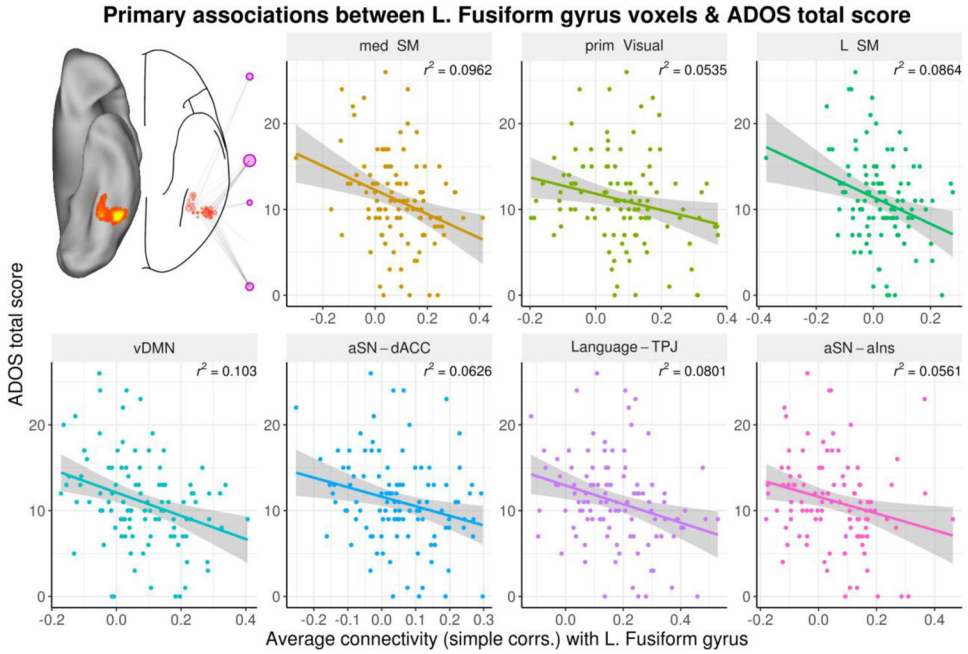

Figure 4.

Scatterplots of associations between Autism Diagnostic Observation Schedule (ADOS) total scores, connectivity with the left fusiform gyrus, and specific intrinsic connectivity networks (ICNs). Connectivity was measured by simple correlations (simple corrs.) between voxel and ICN time series. ADOS total scores were negatively associated with connectivity between the left fusiform gyrus and seven influential ICNs, including the medial and Left Sensorimotor networks (med SM and L SM, respectively), the ventral Default Mode Network (vDMN), and a Language network centered on the bilateral temporoparietal junction (Language-TPJ). Less influential negative associations between ADOS total scores were observed for connectivity between the left fusiform gyrus and the primary Visual network (prim Visual), and anterior Salience Networks centered on the dorsal Anterior Cingulate Cortex (aSN-dACC) and anterior insula (aSN-aIns). The x-axis plots correlations between all voxels included in cluster and each specific ICN, for each subject. The y-axis plots ADOS total scores for each subject. Inset in the top left shows anatomical cluster and connectivity corresponding to the left fusiform gyrus in Figure 2.

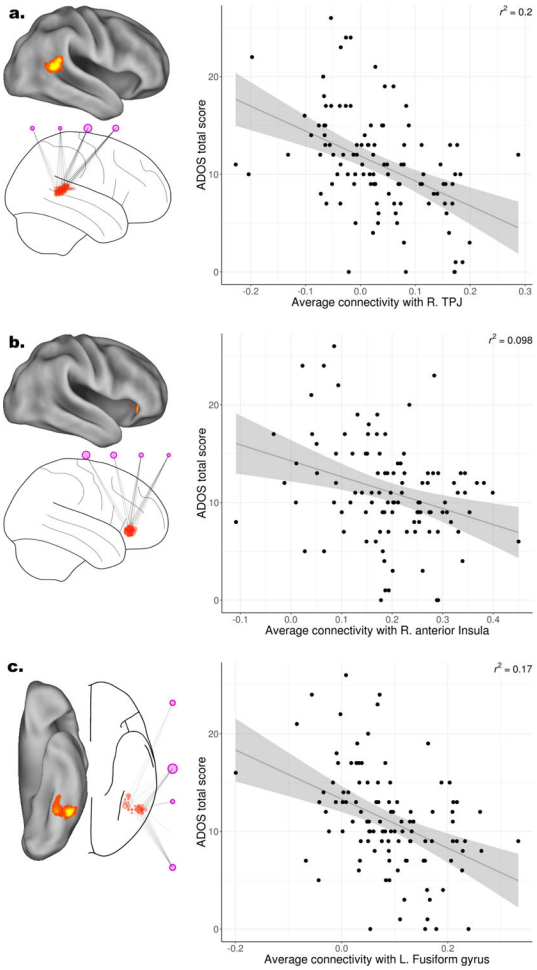

Figure 5.

Directional associations between Autism Diagnostic Observation Schedule (ADOS) total scores and connectivity in select regions. When averaged over all voxels and associated networks in the: **(a.)** right temporoparietal junction (TPJ), **(b.)** right anterior insula, or **(c.)** left fusiform gyrus, decreased connectivity was associated with increased ADOS total scores. For each region, the relevant neuroanatomy and networks are displayed on the left (see Figure 2). On the right, scatterplots of averaged connectivity over all voxels and networks in each subregion are displayed, with regression lines including standard errors and coefficient of variation to assess fit. In all regions and all networks, decreased connectivity was associated with increased ADOS total scores.

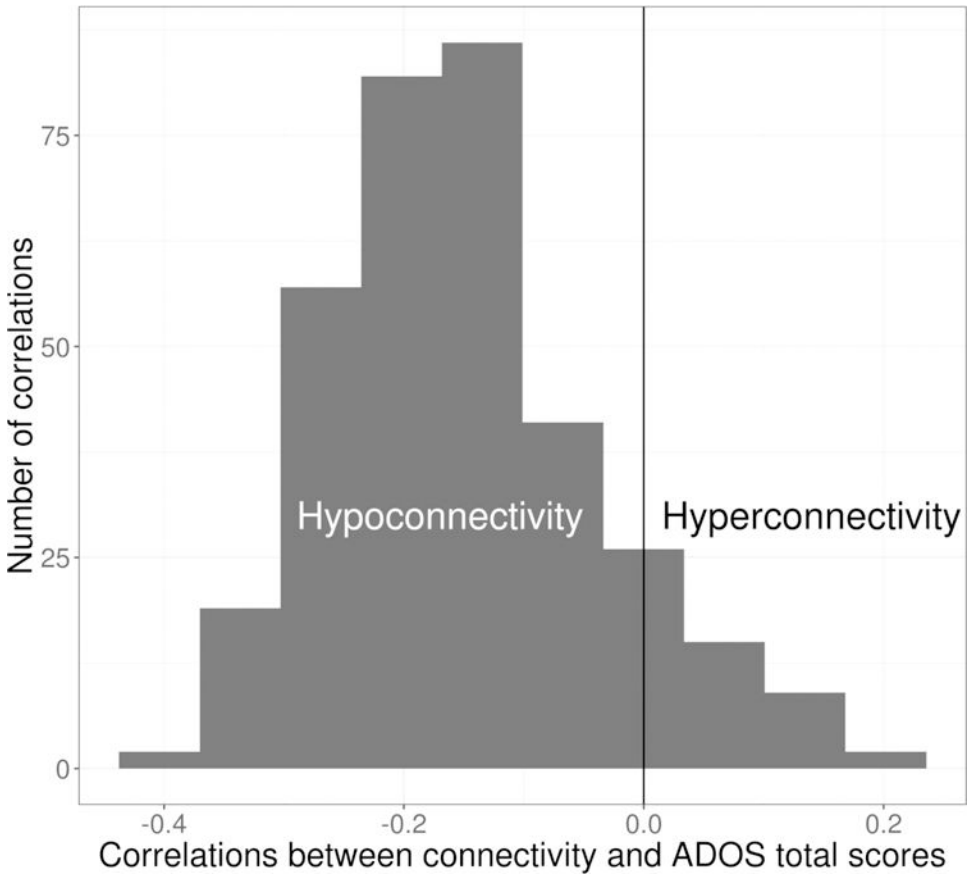

Figure 6.

Autism Diagnostic Observation Schedule (ADOS) total scores are primarily associated with hypoconnectivity. Histogram of the correlation between ADOS total scores and voxel-level connectivity, for all associations displayed in Figure 2 (i.e., all lines connecting a red voxel node to a purple Intrinsic Connectivity Network node), showed predominantly negatively correlations, indicating that decreased connectivity predicts increased ADOS total scores.

Table 1

Sample description

Age (years):	12.9 ± 3.0
Sex (n):	M=89, F=18
Diagnosis (n):	ASD=99, TD=8
Full Scale IQ:	105.1 ± 17.8
Autism Diagnostic Observation Schedule Score:	
Total (n=107):	11.1 ± 5.2
Social Affect (n=101):	8.2 ± 4.1
Restricted/Repetitive Behaviors (n=102):	2.8 ± 1.7

[a] Reported values indicate mean ± standard deviation, unless otherwise noted.

[b] Abbreviations: ASD = autism spectrum disorder; TD = typically developing.

[c] Subjects included from the following sites: New York University Langone Medical Center (n=43), University of Michigan samples 1 (n=24) and 2 (n=10), Utah School of Medicine (n=17), and Yale Child Study Center (n=14).

Table 2

Local peak coordinates of associations with Autism Diagnostic Observation Schedule total scores

Cluster Size (k):	Statistic (dCov):	x	y	z	BA:	AAL Label:
31	1.84	36	27	−3	47	Insula_R
	1.34	33	30	6	48	Insula_R
18	1.74	−42	−75	−15	19	Fusiform_L
	1.57	−36	−81	−9	19	Occipital_Inf_L
57	1.66	48	−45	12	21	Temporal_Mid_R
	1.52	57	−48	12	22	Temporal_Mid_R
	1.51	54	−39	18	42	Temporal_Sup_R
32	1.6	−45	−54	−18	37	Fusiform_L
	1.42	−36	−51	−18	37	Fusiform_L
	1.35	−39	−57	−12	37	Fusiform_L
	1.35	−36	−42	−21	37	Fusiform_L
16	1.56	−42	0	42	6	Precentral_L
	1.46	−36	0	36	6	Precentral_L
26	1.54	24	−42	−6	37	ParaHippocampal_R
	1.4	18	−39	0	27	Lingual_R
	1.4	24	−36	−12	30	Fusiform_R
	1.37	15	−39	−9	30	ParaHippocampal_R
15	1.53	−36	−18	−6	20	Putamen_L
	1.48	−30	−18	−12	20	Hippocampus_L
17	1.5	−3	−51	48	7	Precuneus_L
	1.44	3	−45	51	7	Precuneus_R
31	1.49	−42	3	6	48	Insula_L
	1.45	−33	−12	3	48	Insula_L
	1.43	−36	−3	6	48	Insula_L
17	1.42	42	−6	−36	20	Temporal_Inf_R

[a] Abbreviations: dCov = distance covariance; BA = Brodmann Area; AAL = Automated Anatomical Likelihood atlas; R = right hemisphere; L = left hemisphere; Inf = inferior; Mid = middle; Sup = superior.

[b] Coordinates x ,y, z, are relative to Montreal Neurological Institute (MNI) space.